Biomolecular Nanopatterning

DOI: 10.1002/anie.200803456

Biomolecular Nanopatterning by Magnetic Electric Lithography**

Zhen Gu, Suxian Huang, and Yong Chen**

Biomolecular nanopatterning techniques hold enormous promise for biological and medical applications, including highly sensitive diagnostics, genomics, proteomics,[1] and integrated biomaterials.[2] Numerous lithographic techniques, such as dip-pen nanolithography,[3] nanografting,[4] and electron-beam lithography,[5] have been used to generate biomolecular nanopatterns with high resolution. However, these serial point-to-point lithographic techniques are limited by their low speed in generating nanopatterns over large areas. Parallel lithographic techniques such as nanocontact printing[6] and nanoimprint lithography[7] can generate nanopatterns at high speed over large areas, but it is challenging to incorporate multiple distinct biomolecules into these lithographic processes to generate heterogeneous nanopatterns.[8] Bottom-up self-assembled nanoparticles,[9] copolymers,[10] and DNA oligonucleotides[11] have been employed as templates to guide subsequent assembly of biomolecular nanopatterns, but the fabrication of arbitrary long-range-ordered biomolecular nanopatterns remains elusive. Herein, we present a new facile biomolecular nanopatterning technique, magnetic electric lithography (MEL), to guide the assembly of magnetic nanoparticles (MNPs) coated with distinct biomolecules to form heterogeneous biomolecular nanopatterns on a template at a resolution down to 10 nm. The nanopatterns can be faithfully transferred from the template to a biocompatible polymer substrate for general biomedical applications.

The MEL process is shown in Scheme 1. Water-soluble MNPs coated with distinct biomolecules (proteins or DNA; see the Experimental Section) in deionized water are delivered through a microfluidic system (Scheme 1 a) and deposited onto a template surface within specific areas by applying a magnetic field with a strong gradient from the back side of the template for 20 seconds (Scheme 1 b). The MNPs are subsequently immobilized onto gold nanoelectrodes on the template surface by applying a 1.5 V direct-current potential for five seconds on the nanoelectrodes (Scheme 1 c). The binding between the MNPs and Au nanoelectrodes can

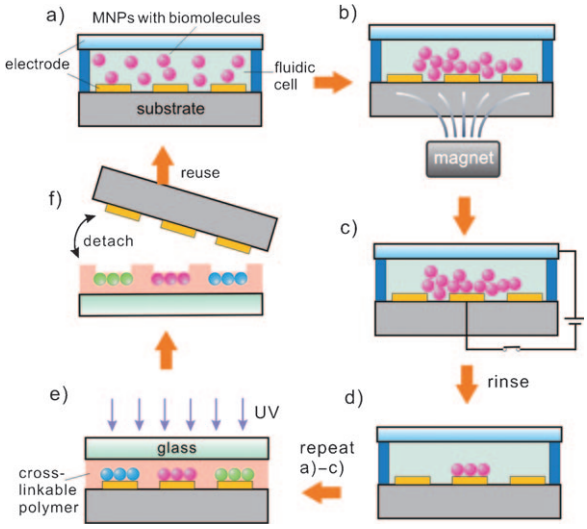

Scheme 1. The magnetic electric lithographic (MEL) process.

be attributed to the electrical neutralization of the charged MNPs.[12] MNPs that are nonspecifically bound to the template surface can be removed by positioning the magnet on the top side of the template and rinsing the template surface (Scheme 1 d). Different MNPs coated with distinct biomolecules can be attracted to the desired area on the template surface and immobilized onto different nanoelectrodes in parallel (Scheme 1 e). The MNP nanopatterns assembled on the template surface are then immersed into an aqueous poly(ethylene glycol) diacrylate (PEG-DA) solution, which can be cross-linked by UV light (Scheme 1 e). After the template is separated from the polymer substrate, the MNP nanopatterns can be completely transferred from the template to the biocompatible PEG hydrogel[13] substrate (Scheme 1 f). The details of the MEL processes are described in the Experimental Section and in the Supporting Information.

Figure 1 displays a series of atomic force microscopy (AFM) images showing the MEL process. 60 nm wide Au nanoelectrodes form the boundaries of the characters "M", "E", and "L" on a SiO_2/Si template surface (Figure 1 a). By sequential application of a 1.5 V potential to the "M", "E", and "L" nanoelectrodes, MNPs coated with three distinct DNA oligonucleotides (S1, S2, and S3; see the Experimental Section) were sequentially immobilized onto the nanoelectrodes (Figure 1 b–d). As measured by AFM, the nanoelectrodes assembled with the MNPs are approximately 20 nm higher than those without MNPs, and there was no obvious immobilization of MNPs beyond the nanoelectrodes to which the electrical potential was applied. After the MNPs were transferred to the PEG polymer substrate, the AFM image of the template surface (Figure 1 e) showed that the nanoelec-

[*] Z. Gu, S. Huang, Prof. Y. Chen
Department of Mechanical and Aerospace Engineering
Department of Biomedical Engineering, California NanoSystems Institute
University of California, Los Angeles, CA 90095 (USA)
Fax: (+1) 310-206-2302
E-mail: guzhen@ucla.edu
yongchen@seas.ucla.edu

[**] This work was supported by the Center on Functional Engineered and Nano Architectonics (FENA) at UCLA, NSF Center for Scalable and Integrated NanoManufacturing (SINAM), and by NIH, through Pacific Southwest Regional Center of Excellence. Dr. Z. Zhu and A. Shen are acknowledged for device measurement and fabrication.

Supporting information for this article is available on the WWW under http://dx.doi.org/10.1002/anie.200803456.

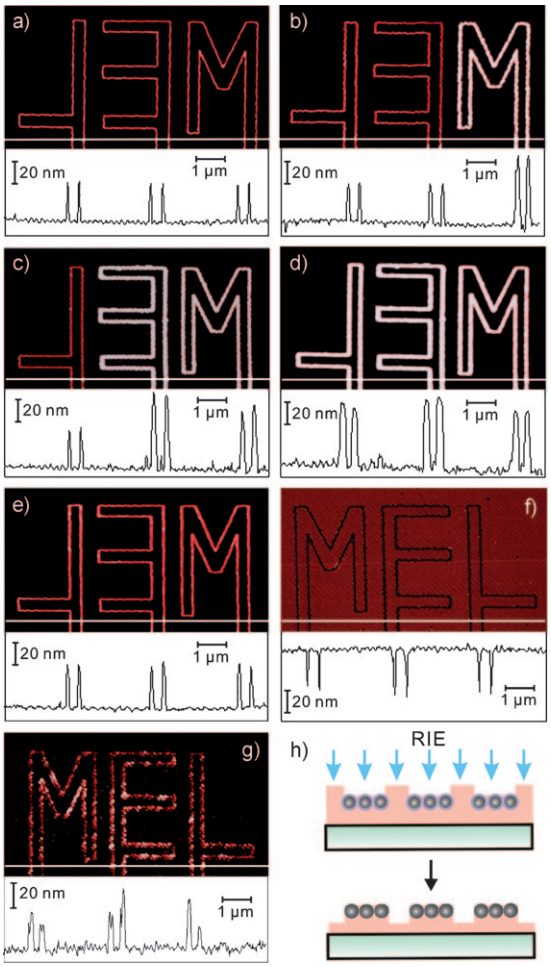

Figure 1. Atomic force microscopy (AFM) images and the corresponding height profiles along the lines on the images showing a) Au nanowire electrodes as the boundaries of characters "M", "E", and "L" on a template surface; b)–d) Magnetic nanoparticles (MNPs) sequentially assembled onto the "M", "E", and "L" nanoelectrodes; e) template and f) polymer surfaces after the MNPs were transferred from the template to the polymer substrate; g) the extruded MNP nanopatterns after the polymer was etched by reactive ion etching (RIE). h) Schematic cross-sectional views of the polymer substrate before and after RIE.

trodes had recovered to the original morphology as shown in Figure 1 a, and the MNPs had been completely transferred to the polymer substrate. The template can be reused many times (see the Supporting Information). The template surface morphology was faithfully embossed onto the polymer substrate (Figure 1 f). After the polymer was selectively etched by reactive ion etching (RIE), the MNPs buried underneath the polymer surface were extruded (Figure 1 g, h), showing the nanopatterns formed by the MNPs.

We have tested the bioactivity and specificity of the biomolecular nanopatterns on the polymer substrate shown in Figure 1 f. The polymer substrate was exposed to a mixed solution of three different fluorophore-labeled DNA oligonucleotides (F1, F2, and F3; see the Experimental Section) that are complementary to the aforementioned S1, S2, and S3 DNA strands coated on the MNPs. A superimposed fluorescence image of the complementary DNA nanopatterns after DNA hybridization is shown in Figure 2 a. Although the fluorescent nanopatterns are blurred owing to the resolution limit of the fluorescence microscope (see the Supporting Information), the image still indicates the specific hybridization between the DNA strands and the reactivity and specificity of the DNA on the MNPs (Figure 2 b).

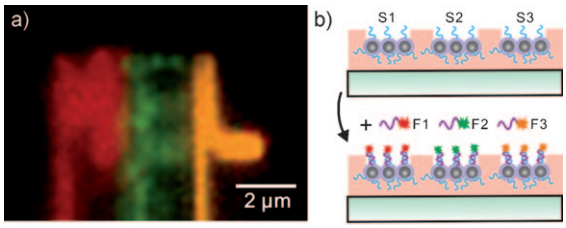

Figure 2. a) A superimposed fluorescence image and b) schemes showing that the fluorophore-labeled complementary DNA oligonucleotides (F1, F2, and F3) are conjugated with the DNA strands (S1, S2, and S3) on the MNP nanopatterns on the PEG polymer substrate shown in Figure 1 f.

To demonstrate the high resolution of MEL, a template consisting of two parallel 8 nm wide Au nanoelectrodes was fabricated on a SiO_2 surface (see Figure 3 a and the Experimental Section). Streptavidin-coated single MNPs with a diameter of approximately 10 nm were immobilized and aligned in a row along the Au nanoelectrodes by MEL (Figure 3 b). The MNPs were coated with streptavidin labeled with green fluorophores (Alexa Fluor 488); therefore, a green fluorescent line can be observed along the nanoelectrodes by the fluorescence microscope (Figure 3 c), but the double nanoelectrodes cannot be distinguished owing to the limita-

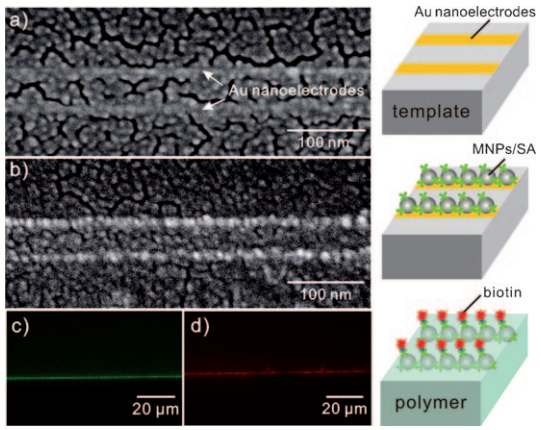

Figure 3. Scanning electron microscopy (SEM) images of a) two parallel 8 nm wide Au nanoelectrodes on a template; and b) streptavidin (SA)-coated 10 nm MNPs immobilized on the Au nanoelectrodes. The template surfaces were coated with a 2 nm thick Au film to eliminate charge effects during the SEM observation. Fluorescence microscopy images of c) green-fluorophore-labeled streptavidin on MNPs immobilized along the Au nanowires on the template; and d) red-fluorophore-labeled biotin after reaction with the streptavidin on the MNPs transferred to a PEG polymer substrate. The corresponding MEL process is shown schematically in the right column.

tion of the microscope resolution. After the MNPs were transferred to a PEG polymer substrate, the streptavidin units on the MNPs were treated with biotin labeled with a red fluorophore (Atto-590). A red fluorescent line can then be observed along the nanoelectrodes (Figure 3d). The experimental results indicate that MEL can generate biomolecular nanopatterns with a resolution down to approximately 10 nm. The resolution is defined by the sizes of the MNPs and of the nanoelectrodes on the template.

To explore biomolecular nanopatterns by a parallel MEL process over a large area, we fabricated a template with an array of nanoholes through a SiO_2 layer over an area of approximately 0.5 cm^2, and microscale Au electrodes buried underneath the SiO_2 layer were exposed to the template surface through the nanoholes (Figure 4a). Different MNPs

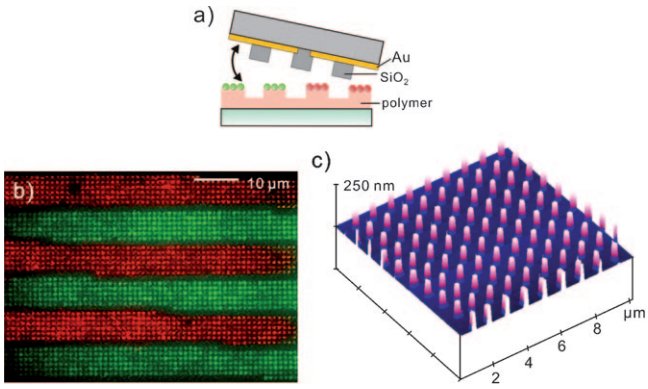

Figure 4. a) An MEL template and parallel process to fabricate heterogeneous biomolecular nanopatterns over a large area. A superimposed fluorescence image (b) and an AFM image (c) showing a nanoarray of streptavidin-coated MNPs labeled with red and green fluorophores on a PEG polymer substrate.

coated with streptavidin labeled with a red (Alexa Fluor 594) or a green (Alexa Fluor 488) fluorophore were delivered to the template surface through the microfluidic system. A 1.5 V potential was applied for five seconds on the Au electrodes to immobilize the different MNPs onto the different Au electrodes through the SiO_2 nanoholes over the whole template surface in parallel. The MNPs were then transferred to a PEG polymer substrate. Fluorescence and AFM images of the MNP nanoarray on the polymer substrate are shown in Figure 4b,c, which indicates that heterogeneous biomolecular nanoarrays can be facilely fabricated over a large area by a parallel MEL process.

In essence, we have developed a magnetic electric lithography (MEL) technique, in which MNPs coated with multiple distinct biomolecules can be conveniently delivered through a microfluidic system, rapidly deposited onto a template surface within specific areas by a magnetic field, and selectively immobilized onto the nanoelectrodes by applying an electric potential on the electrodes. Heterogeneous biomolecular nanopatterns formed by the MNPs assembled on the nanoelectrodes can be reliably transferred to a biocompatible polymer substrate. We have demonstrated that nanopatterns with a resolution down to approximately 10 nm can be fabricated by MEL, and heterogeneous biomolecular nanoarrays can be obtained by a parallel MEL process over an area of approximately 0.5 cm^2 within two minutes. The resolution can potentially be improved by further reducing the sizes of MNPs and nanoelectrodes on the template. An integrated MEL system with dynamically controlled magnetic field, electric potential, and multiple microfluidic channels can potentially fabricate complex biomolecular nanopatterns on demand with high resolution, speed, and throughput for various biological and medical applications.

Experimental Section

Water-soluble iron oxide (Fe_3O_4) MNPs with an average diameter of approximately 10 nm were synthesized and capped with positively charged 2-pyrrolidinone,[14] and a negatively charged poly(styrene sulfonate) (PSS) layer was then self-assembled onto the MNPs.[15] Streptavidin was physically adsorbed to the PSS-coated MNPs,[16] and three different biotinylated DNA oligonucleotides (S1, S2, and S3, Table 1) were conjugated with the streptavidin on the MNPs (see the Supporting Information). The cross-linkable polymer solution for MNP transfer contains 66 wt% poly(ethylene glycol) diacrylate (PEG-DA, $n = 400$), 3.0 wt% 2-hydroxy-4-(2-hydroxyethoxy)-2-methylpropiophenone as photoinitiator, 30 wt% phosphate-buffered saline (PBS), and 1 wt% surfactant (Tween-20). The PEG polymer solution was cross-linked by UV exposure with an intensity of 11.0 mW cm^{-2} for 30 seconds to form PEG hydrogel. After the MNPs were transferred to the PEG polymer substrate, complementary DNA strands (F1, F2, and F3, Table 1) were hybridized with the DNA on the MNPs in a buffer solution (1M NaCl, 10 mM 2-amino-2-hydroxymethyl-propane-1,3-diol (tris) HCl, 1 mM ethylenediamine tetraacetic acid (EDTA), and 0.01% (w/v) sodium dodecyl sulfate (SDS), pH 7.4) at room temperature (25°C) for 12 h. The biotin was conjugated with the streptavidin on the MNPs in a solution of 10 μg mL^{-1} biotin in PBS solution for 1 hour.

Table 1: DNA sequences used in this study.

Code	Sequence	λ ex[a]/em[b] [nm]
S1	5′-biotin-T_{15} GCTTATCGAGCTTTCG-3′	
S2	5′-biotin-T_{15} ATCGATCGAGCTGCAA-3′	
S3	5′-biotin-T_{15} ATCAGTGCAGGAGCTA-3′	
F1	5′-TEX613-CGAAAGCTCGATAAGC-3′	596/613
F2	5′-FAM-TTGCAGCTCGATCGAT-3′	495/520
F3	5′-Cy3-TAGCTCCTGCACTGAT-3′	550/564

[a] The maximum excitation wavelengths. [b] The maximum emission wavelengths.

Received: July 17, 2008
Published online: November 12, 2008

Keywords: biomolecules · gels · immobilization · lithography · nanomaterials

[1] a) J. M. Nam, S. W. Han, K. B. Lee, X. Liu, M. A. Ratner, C. A. Mirkin, *Angew. Chem.* **2004**, *116*, 1266–1269; *Angew. Chem. Int. Ed.* **2004**, *43*, 1246–1249; b) R. A. Vega, D. Maspoch, K. Salaita, C. A. Mirkin, *Angew. Chem.* **2005**, *117*, 6167–6169; *Angew. Chem. Int. Ed.* **2005**, *44*, 6013–6015.

[2] a) J. M. Anderson, T. L. Bonfield, N. P. Ziats, *Int. J. Artif. Organs* **1990**, *13*, 375–382; b) W. H. Koch, *Nat. Rev. Drug Discovery*

2004, *3*, 749 – 761; c) J. R. Capadona, T. A. Petrie, K. R. Fears, R. A. Latour, D. M. Collard, A. S. J. Garcia, *Adv. Mater.* **2005**, *17*, 2604 – 2608; d) K. B. Lee, E. Y. Kim, C. A. Mirkin, S. M. Wolinsky, *Nano Lett.* **2004**, *4*, 1869 – 1872; e) W. Senaratne, P. Sengupta, V. Jakubek, D. Holowka, C. K. Ober, B. Baird, *J. Am. Chem. Soc.* **2006**, *128*, 5594 – 5595; f) N. Walter, C. Selhuber, H. Kessler, J. P. Spatz, *Nano Lett.* **2006**, *6*, 398 – 402.

[3] a) K. B. Lee, S. J. Park, C. A. Mirkin, J. C. Smith, M. Mrksich, *Science* **2002**, *295*, 1702 – 1705; b) J. Hyun, S. J. Ahn, W. K. Lee, A. Chilkoti, S. Zauscher, *Nano Lett.* **2002**, *2*, 1203 – 1207; c) D. L. Wilson, R. Martin, S. Hong, M. Cronin-Golomb, C. A. Mirkin, D. L. Kaplan, *Proc. Natl. Acad. Sci. USA* **2001**, *98*, 13660 – 13664.

[4] K. Wadu-Mesthrige, S. Xu, N. A. Amro, G. Y. Liu, *Langmuir* **1999**, *15*, 8580 – 8583.

[5] a) Y. Hong, P. Krsko, M. Libera, *Langmuir* **2004**, *20*, 11123 – 11126; b) D. Klinov, K. Atlasov, A. Kotlyar, B. Dwir, E. Kapon, *Nano Lett.* **2007**, *7*, 3583 – 3587.

[6] a) J. P. Renault, A. Bernard, A. Bietsch, B. Michel, H. R. Bosshard, E. Delamarche, M. Kreiter, B. Hecht, U. P. Wild, *J. Phys. Chem. B* **2003**, *107*, 703 – 711; b) H. W. Li, B. V. O Muir, G. Fichet, W. T. S. Huck, *Langmuir* **2003**, *19*, 1963 – 1965.

[7] J. D. Hoff, L. J. Cheng, E. Meyhofer, L. J. Guo, A. J. Hunt, *Nano Lett.* **2004**, *4*, 853 – 857.

[8] S. R. Coyer, A. J. Garcia, E. Delamarche, *Angew. Chem.* **2007**, *119*, 6961 – 6964; *Angew. Chem. Int. Ed.* **2007**, *46*, 6837 – 6840.

[9] Y. Cai, B. M. Ocko, *Langmuir* **2005**, *21*, 9274 – 9279.

[10] J. M. Jung, K. Y. Kwon, T. H. Ha, B. H. Chung, H. T. Jung, *Small* **2006**, *2*, 1010 – 1015.

[11] H. Yan, S. H. Park, G. Finkelstein, J. H. Reif, T. H. LaBean, *Science* **2003**, *301*, 1882 – 1884.

[12] a) O. O. Van der Biest, L. J. Vandeperre, *Annu. Rev. Mater. Sci.* **1999**, *29*, 327 – 352; b) R. C. Hayward, D. A. Saville, I. A. Aksay, *Nature* **2000**, *404*, 56 – 59; c) E. Kumacheva, R. K. Golding, M. Allard, E. H. Sargent, *Adv. Mater.* **2002**, *14*, 221; d) S. R. Yeh, M. Seul, B. I. Shraiman, *Nature* **1997**, *386*, 57 – 59; e) P. Mesquida, A. Stemmer, *Adv. Mater.* **2001**, *13*, 1395 – 1398.

[13] a) D. J. Beebe, J. S. Moore, J. M. Bauer, Q. Yu, R. H. Liu, C. Devadoss, B. H. Jo, *Nature* **2000**, *404*, 588 – 590; b) A. Khademhosseini, J. Yeh, S. Jon, G. Eng, K. Y. Suh, J. A. Burdick, R. Langer, *Lab Chip* **2004**, *4*, 425 – 430; c) D. C. Pregibon, M. Toner, P. Doyle, *Langmuir* **2006**, *22*, 5122 – 5512; d) D. C. Pregibon, M. Toner, P. Doyle, *Science* **2007**, *315*, 1393 – 1396.

[14] Z. Li, H. Chen, H. Bao, M. Y. Gao, *Chem. Mater.* **2004**, *16*, 1391 – 1393.

[15] a) G. Schneider, G. Decher, *Nano Lett.* **2004**, *4*, 1833 – 1839; b) G. Schneider, G. Decher, N. Nerambourg, R. Praho, M. H. V. Werts, M. Blanchard-Desce, *Nano Lett.* **2006**, *6*, 530 – 536.

[16] a) W. Norde, J. Lyklema, *J. Colloid Interface Sci.* **1979**, *71*, 350 – 366; b) B. D. Fair, A. M. Jamieson, *J. Colloid Interface Sci.* **1980**, *77*, 525 – 534; c) D. Song, D. Forciniti, *J. Colloid Interface Sci.* **2000**, *221*, 25 – 37; d) A. Gessner, B. R. Paulke, R. H. Muller, *Electrophoresis* **2000**, *21*, 2438 – 2442; e) H. Sun, N. Hu, *Biophys. Chem.* **2004**, *110*, 297 – 308; f) D. Lazos, S. Franzka, M. Ulbricht, *Langmuir* **2005**, *21*, 8774 – 8784.

